Atomic Quantum Simulation of Dynamical Gauge Fields Coupled to Fermionic Matter: From String Breaking to Evolution after a Quench

D. Banerjee,[1] M. Dalmonte,[2,3] M. Müller,[4] E. Rico,[2,3] P. Stebler,[1] U.-J. Wiese,[1] and P. Zoller[2,3,5]

[1]*Albert Einstein Center, Institute for Theoretical Physics, Bern University, CH-3012, Bern, Switzerland*

[2]*Institute for Quantum Optics and Quantum Information of the Austrian Academy of Sciences, A-6020 Innsbruck, Austria*

[3]*Institute for Theoretical Physics, Innsbruck University, A-6020 Innsbruck, Austria*

[4]*Departamento de Fisica Teorica I, Universidad Complutense, 28040 Madrid, Spain*

[5]*Joint Quantum Institute: National Institute of Standards and Technology, and University of Maryland, College Park, Maryland 20742, USA*

(Received 29 May 2012; revised manuscript received 9 August 2012; published 23 October 2012)

Using a Fermi-Bose mixture of ultracold atoms in an optical lattice, we construct a quantum simulator for a $U(1)$ gauge theory coupled to fermionic matter. The construction is based on quantum links which realize continuous gauge symmetry with discrete quantum variables. At low energies, quantum link models with staggered fermions emerge from a Hubbard-type model which can be quantum simulated. This allows us to investigate string breaking as well as the real-time evolution after a quench in gauge theories, which are inaccessible to classical simulation methods.

DOI: 10.1103/PhysRevLett.109.175302 PACS numbers: 67.85.−d, 11.15.Ha, 37.10.Vz, 75.10.Jm

Recently, the condensed matter and atomic physics communities have mutually benefited from synergies emerging from the quantum simulation of strongly correlated systems using atomic setups [1–4]. In particular, physically interesting quantum many-body systems, which can not be solved with classical simulation methods, are becoming accessible to analog or digital quantum simulation with cold atoms, molecules, and ions. In the future, quantum simulators may also enable us to address currently unsolvable problems in particle physics, including the real-time evolution of the hot quark-gluon plasma emerging from a heavy-ion collision or the deep interior of neutron stars [5].

The challenge on the atomic physics side is to find a physical implementation of gauge theories with cold atoms, and to identify possible atomic setups representing dynamical gauge fields coupled to fermionic matter. Below we provide a toolbox for a $U(1)$ lattice gauge theory (LGT) using atoms in optical lattices [1,3]. Here fermionic atoms represent matter fields. They hop between lattice sites and interact with dynamical gauge fields on the links embodied by bosonic atoms. The LGT to be implemented is a so-called quantum link model (QLM) [6–8], where the fundamental gauge variables are represented by quantum spins. QLMs extend the concept of Wilson's LGT [9]. In particle physics they provide an alternative nonperturbative formulation of dynamical Abelian and non-Abelian gauge field theories [8,10,11]. QLMs are also relevant in condensed matter contexts, like spin liquids and frustrated systems [12–14]. Their Hamiltonian formulation provides a natural starting point for quantum simulation protocols based on atomic gases in optical lattices [15–19]. We will illustrate atomic quantum simulation of an Abelian QLM in a 1D setup, demonstrating both dynamical string breaking and the real-time evolution after a quench, which are also relevant in QCD. The quantum simulator discussed below makes the corresponding real-time dynamics, which is exponentially hard for classical simulations based on Wilson's paradigm [20], accessible to atomic experiments.

Cold quantum gases provide a unique experimental platform to study many-body dynamics of isolated quantum systems. In particular, cold atoms in optical lattices realize Hubbard dynamics for both bosonic and fermionic particles, where the single particle and interaction terms can be engineered by external fields. The remarkable experimental progress is documented by the quantitative determination of phase diagrams in strongly interacting regimes, the study of quantum phase transitions, and nonequilibrium quench dynamics [21–25]. One of the most exciting recent developments are *synthetic gauge fields with atoms*, which promise the realization of strongly correlated many-body phases, such as, e.g., the fractional quantum Hall effect with atoms [26–31]. A fermion that is annihilated by ψ_y and recreated by $\psi_x^\dagger$ at a neighboring site x, which propagates in the background of a classical Abelian vector potential $\vec{A}$ gives rise to the hopping term $\psi_x^\dagger u_{xy} \psi_y$ with $u_{xy} = \exp(i\varphi_{xy})$. Hopping between the adjacent lattice sites x and y accumulates the phase $\varphi_{xy} = \int_x^y d\vec{l} \cdot \vec{A}$. The hopping term is invariant against $U(1)$ gauge transformations $\vec{A}' = \vec{A} - \vec{\nabla}\alpha$ [32,33]. When a fermion hops around a lattice plaquette $\langle wxyz \rangle$, it picks up a gauge invariant magnetic flux phase $\exp(i\Phi) = u_{wx}u_{xy}u_{yz}u_{zw}$, with $\Phi = \int d^2\vec{f} \cdot \vec{\nabla} \times \vec{A}$. We emphasize that these synthetic gauge fields are c numbers mimicking an external magnetic field for the (neutral) atoms.

Instead, here we are interested in *dynamical* gauge fields as they arise in particle physics [34]. The corresponding fundamental bosonic degrees of freedom U_{xy} are no longer related to an underlying classical background field $\vec{A}$, but represent quantum operators associated with the lattice links. The hopping of the fermions is now mediated by the bosonic gauge field via the term $\psi_x^\dagger U_{xy}\psi_y$, which is invariant under local changes of matter and gauge degrees of freedom $U'_{xy} = V^\dagger U_{xy} V = \exp(i\alpha_x) U_{xy} \exp(-i\alpha_y)$, $\psi'_x = V^\dagger \psi_x V = \exp(i\alpha_x)\psi_x$, $V = \prod_x \exp(i\alpha_x G_x)$, and $G_x = \psi_x^\dagger \psi_x - \sum_i (E_{x,x+\hat{i}} - E_{x-\hat{i},x})$. Here $E_{x,x+\hat{i}}$ is an electric field operator associated with the link connecting x and $y = x + \hat{i}$, where $\hat{i}$ is a unit-vector in the i direction. G_x is the generator of gauge transformations (see Supplemental Material [33] for a detailed discussion). Gauge invariant physical states must obey Gauss' law, $G_x|\Psi\rangle = 0$, which is the lattice variant of $\vec{\nabla}\cdot\vec{E} = \rho = \psi^\dagger\psi$. To ensure gauge covariance of U_{xy}, it must obey $[E_{xy}, U_{xy}] = U_{xy}$. The Hamiltonian representing the electric and magnetic field energy of a compact $U(1)$ LGT, $H = \frac{g^2}{2}\sum_{\langle xy\rangle} E_{xy}^2 - \frac{1}{4g^2}\sum_{\langle wxyz\rangle} (U_{wx}U_{xy}U_{yz}U_{zw} + \text{H.c.})$, is gauge invariant, i.e., $[H, G_x] = 0$. In Wilson's LGT, the link variables $U_{xy} = \exp(i\varphi_{xy}) \in U(1)$ are still complex phases, and $E_{xy} = -i\partial/\partial\varphi_{xy}$. Since U_{xy} is a continuous variable, which implies an infinite-dimensional Hilbert space per link, it is not clear how to implement it in ultracold matter, where one usually deals with discrete degrees of freedom in a finite-dimensional Hilbert space.

Quantum link models offer an attractive framework for the quantum simulation of dynamical gauge fields [8,10,11]. They extend the concept of a LGT to systems of discrete quantum degrees of freedom with only a finite-dimensional Hilbert space per link. In contrast to the Wilson formulation, QLMs resemble a quantum rather than a classical statistical mechanics problem. The relation $[E_{xy}, U_{xy}] = U_{xy}$ is then realized by a quantum link operator $U_{xy} = S_{xy}^+$ which is a raising operator for the electric flux $E_{xy} = S_{xy}^3$ associated with the link connecting neighboring lattice sites x and y. A local $SU(2)$ algebra is generated by a quantum spin $\vec{S}_{xy}$ with just $2S + 1$ states per link (see Ref. [33]). We will consider quantum links with $S = \frac{1}{2}$ or 1. In the classical limit $S \to \infty$ QLMs reduce to the Hamiltonian formulation [35,36] of Wilson's LGT.

The implementation of quantum link models in ultracold matter requires the realization of a gauge invariant Hamiltonian accompanied by the corresponding Gauss law. Here, we present a general procedure to obtain $U(1)$ QLMs including both gauge and matter fields. To illustrate our method, we focus on a simple example, a 1D $U(1)$ QLM coupled to so-called staggered fermions with the Hamiltonian

$$H = -t\sum_x [\psi_x^\dagger U_{x,x+1}\psi_{x+1} + \text{H.c.}] + m\sum_x (-1)^x \psi_x^\dagger\psi_x + \frac{g^2}{2}\sum_x E_{x,x+1}^2. \quad (1)$$

Here t is the hopping parameter [see Fig. 1(a)], m is the fermion mass, and g is the gauge coupling. In this case, the gauge generator is given by $\tilde{G}_x = G_x + \frac{1}{2}[(-1)^x - 1]$. Staggered fermions are analogous to spinless fermions at half-filling in condensed matter physics. The corresponding vacuum represents a filled Dirac sea of negative energy states. For $S = 1$, $t = 0$, and $m > 0$ the vacuum state has $E_{x,x+1} = 0$ and $\psi_x^\dagger\psi_x = \frac{1}{2}[1 - (-1)^x]$. The corresponding vacuum energy of a system with L sites is $E_0 = -mL/2$. The above Hamiltonian resembles the Schwinger model [37]. For $S = 1$ it shares the nonperturbative phenomenon of string breaking by dynamical $q\bar{q}$ pair creation with QCD [38]. An external static quark-antiquark pair $\bar{Q}Q$ (with the Gauss law appropriately taken into account) is connected by a confining electric flux string [Fig. 1(c), top], which manifests itself by a large value of the electric flux. For $t = 0$, the energy of this state is $E_{\text{string}} - E_0 = g^2(L-1)/2$, and the flux is given by $\langle\sum_x E_{x,x+1}\rangle = -L + 1$. At sufficiently large L, the string's potential energy is converted into kinetic energy by fermion hopping, which amounts to the creation of a dynamical quark-antiquark pair $q\bar{q}$. In this process, which is known as string breaking, an external static antiquark $\bar{Q}$ pairs up with a dynamical quark to form a $\bar{Q}q$ meson. For $t = 0$, the resulting two-meson state of Fig. 1(c) (bottom) has an energy $E_{\text{mesons}} - E_0 = g^2 + 2m$ and a small flux $\langle\sum_x E_{x,x+1}\rangle = -2$. The

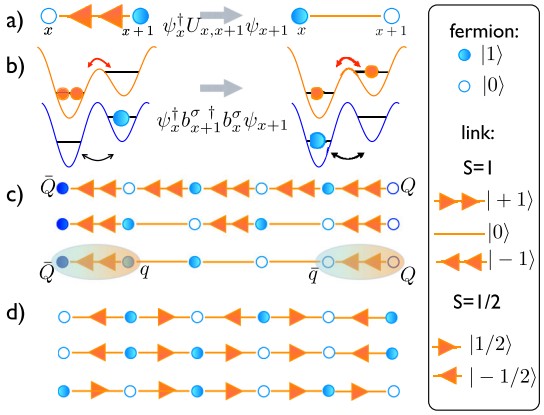

FIG. 1 (color online). (a) Correlated hop of a fermion assisted by $U_{x,x+1} \equiv S_{x,x+1}^+$ consistent with Gauss' law in a QLM with spin $S = 1$. (b) Realization of the process in (a) with bosonic and fermionic atoms in an optical superlattice (see text). (c) Breaking of a string connecting a static $\bar{Q}Q$ pair: from an unbroken string (top), via fermion hopping (middle), to two mesons separated by vacuum (bottom). (d) From a parity-invariant staggered flux state (top), via fermion hopping (middle), to the vacuum with spontaneous parity breaking.

energy difference $E_{\text{string}} - E_{\text{mesons}} = g^2(L-3)/2 - 2m = 0$ determines the length $L = 4m/g^2 + 3$ at which the string breaks.

Another nonperturbative process of interest in particle physics is the real-time evolution after a quench. In particular, the quark-gluon plasma created in a heavy-ion collision quickly returns to the ordinary hadronic vacuum. This is accompanied by the spontaneous breakdown of the quark's chiral symmetry. The dynamics after a quench can be quantum simulated by using the $S = \frac{1}{2}$ representation for the electric flux (which mimics the Schwinger model at vacuum angle $\theta = \pi$ [37]). In that case, like chiral symmetry in QCD, for $m > 0$ parity is spontaneously broken, at least for small t, for more details see Supplemental Material [33]. A quenched parity-invariant staggered flux state, which evolves into the true vacuum with spontaneous parity breaking, is schematically illustrated in Fig. 1(d). In this case, the electric flux represents an order parameter for spontaneous parity breaking, which is expected to perform coherent oscillations. This is similar to the time evolution after a quench starting from a disoriented chiral condensate in QCD [39].

The realization of an atomic LGT simulator requires (i) the identification of physical degrees of freedom to represent fermionic particles and bosonic quantum link variables, (ii) to impose the Gauss law in order to remove the gauge variant states, and (iii) to design the desired dynamics in the gauge invariant subspace. Below we develop a rather general atomic toolbox to implement $U(1)$ lattice gauge models coupled to matter fields based on mixtures of cold fermionic and bosonic atoms in optical lattices. Within this toolbox, we consider two different microscopic realizations in terms of Hubbard models, model I and II. Below we present in some detail the conceptually simpler model I (see Fig. 2), which assumes two-component bosons representing gauge fields. Model II, discussed in the Supplemental Material [33], assumes one component bosons with magnetic or electric dipolar interactions; it offers better scalability and experimental feasibility. Our concepts generalize immediately to experiments in 2D and 3D, and to fermions with spin [33]. (i) The spin $S = \frac{1}{2}, 1, \ldots$ representing the quantum link can be realized with a fixed number $N = 2S$ of bosonic atoms in a double well potential with tunnel coupling [Fig. 1(b)]. An optical superlattice [40,41] (Fig. 2) provides an array of double wells with different depths, and a Mott insulator phase of bosons allows loading with the desired number of atoms N. For two neighboring sites x and $x+1$, with b_x^σ and b_{x+1}^σ denoting the boson destruction operators in the corresponding wells, we define a Schwinger representation for the quantum link

$$U_{x,x+1} = b_{x+1}^{\sigma\dagger} b_x^\sigma, \; E_{x,x+1} = \frac{1}{2}(b_{x+1}^{\sigma\dagger} b_{x+1}^\sigma - b_x^{\sigma\dagger} b_x^\sigma). \qquad (2)$$

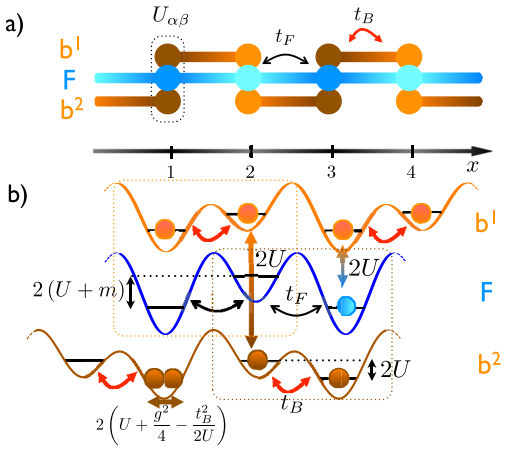

FIG. 2 (color online). Schematic view of the optical superlattices for one fermionic and two bosonic species 1 and 2 (model I). (a) Species 1 can hop between an even site x and the odd site $x-1$, while species 2 can hop between x and $x+1$. (b) Illustration of various contributions to the Hamiltonian. Fermions and two-component bosons have on-site repulsions $U_{1F} = U_{2F} = U_{12} = 2U$, while bosons of the same species have $U_{11} = U_{22} = 2U + g^2/2 - t_B^2/U$. The offsets of the bosonic and fermionic superlattices are $2U_1 = 2U_2 = 2U$ and $2U_F = 2(U+m)$, respectively. If the fermion hops to the left, it picks up the energy offset $2U$ from a boson of species 2 which simultaneously tunnels to the right.

The electric flux is related to the population difference of the two sites. Here the bosonic species index $\sigma = 1, 2$ distinguishes between links originating from even and odd sites x. Equation (2) requires that each boson can tunnel only to one specific neighboring site, based on a term $h^B_{x,x+1} = -t_B b_{x+1}^{\sigma\dagger} b_x^\sigma + \text{H.c.}$ The number of bosonic atoms is conserved locally on each link. In the Supplemental Material [33] we discuss model II with just a single bosonic species, by encoding σ in the geometric location of the bosons to the left or to the right of the site x. We now also add spinless fermionic atoms at half-filling to our superlattice setup, which can hop between neighboring sites based on the term $h^F_{x,x+1} = -t_F \psi_{x+1}^\dagger \psi_x + \text{H.c.}$ (ii) Gauss law: Using $b_x^{\sigma\dagger} b_x^\sigma + b_{x+1}^{\sigma\dagger} b_{x+1}^\sigma = 2S$, the gauge generator reduces to

$$\tilde{G}_x = n_x^F + n_x^1 + n_x^2 - 2S + \frac{1}{2}[(-1)^x - 1]. \qquad (3)$$

Here n_x^α counts the atoms of type $\alpha = F, 1, 2$. Up to an x-dependent constant, $\tilde{G}_x$ thus counts the total number of atoms at the site x. To impose the Gauss law, we consider interaction terms which can be rewritten in the form $U\tilde{G}_x^2$ as the dominant term in the Hamiltonian, so that all gauge variant states are removed from the low-energy sector. This is reminiscent of the repulsive Hubbard model for a Mott insulator [1]. In this sense, the gauge invariant states (which obey $n_x^F + n_x^1 + n_x^2 = 2S + \frac{1}{2}[1 - (-1)^x]$) can be viewed as *super-Mott* states. (iii) It is well known that, for

large on-site repulsion, the Hubbard model reduces to the t-J model [42]. We now induce the dynamics of a $U(1)$ QLM in a similar manner, by considering the 1D microscopic Hamiltonian $\tilde{H} = \sum_x h^B_{x,x+1} + \sum_x h^F_{x,x+1} + m\sum_x (-1)^x n^F_x + U\sum_x \tilde{G}^2_x$. Up to an additive constant, it can be expressed as

$$\tilde{H} = -t_B \sum_{x\ \mathrm{odd}} b^{1\dagger}_x b^1_{x+1} - t_B \sum_{x\ \mathrm{even}} b^{2\dagger}_x b^2_{x+1} - t_F \sum_x \psi^\dagger_x \psi_{x+1} + \mathrm{H.c.} + \sum_{x,\alpha,\beta} n^\alpha_x U_{\alpha\beta} n^\beta_x + \sum_{x,\alpha} (-1)^x U_\alpha n^\alpha_x. \quad (4)$$

The last two terms describe repulsive on-site interactions as well as superlattice offsets, and form the basic building block for the Gauss term $U\sum_x \tilde{G}^2_x$. The various contributions to the Hamiltonian are illustrated in Fig. 2(b). The QLM of Eq. (1) with $t = t_B t_F/U$ emerges in second order perturbation theory, if one tunes the parameters to the values listed in Fig. 2(b). The offsets U_α give rise to an alternating superlattice for both the fermions and the bosons. In analogy to superexchange interactions [41], energy conservation enforces a *correlated hop* of the fermion with the spin-flip on the link, thus realizing the term $-t\psi^\dagger_x U_{x,x+1}\psi_{x+1}$. This is the key ingredient for the coupling of fermions and quantum links. Additionally, a gauge invariant term $\delta_F \sum_x \psi^\dagger_x \psi_x [1 - \psi^\dagger_{x+1}\psi_{x+1}]$ is also generated [33]. The reduction of the microscopic model of Eq. (4) to the QLM of Eq. (1) has been verified both at the few- and many-body level, is schematically illustrated in Figs. 3(a) and 3(b), and is extensively discussed in Ref. [33].

We have performed exact diagonalizations on small system sizes to quantitatively show the physical phenomena of string breaking and the dynamics after a quench which can be observed in an experiment. The main results are presented in Figs. 3(c) and 3(d). For $S = 1$, we evolve a *string state* initially prepared as in Fig. 1(c) under Hamiltonian parameters such that the separation between charge and anticharge is larger than the characteristic scale for string breaking $L = 4m/g^2 + 3$. Indeed, the large negative electric flux initially stored in the string quickly approaches its vacuum value, illustrating the string breaking mechanism. For $S = \frac{1}{2}$, Fig. 3(d) also shows the time evolution after a quench, starting from the parity-invariant state at the top of Fig. 1(d). In fact, the electric flux, which is an order parameter for spontaneous parity breaking, displays coherent oscillations, reminiscent of a disoriented chiral condensate in QCD [39]. A general experimental implementation, which will require three basic steps (preparation of an initial gauge invariant state, evolution via quantum link dynamics, and measurement of relevant physical observables), is discussed in the Supplemental Material [33].

In the present Letter, we have proposed a quantum simulator of lattice gauge theories, where bosonic gauge fields are coupled to fermionic matter, allowing demonstration experiments for phenomena such as time-dependent string breaking and the dynamics after a quench. While the basic elements behind our model have been demonstrated individually in the laboratory, the combination of these tools and the extension to higher dimensions remain a challenge to be tackled in future generations of optical lattice experiments. While building a QCD quantum simulator to address questions related to nonzero baryon density and real-time evolution remains a long term goal, we see no fundamental obstacles on the atomic physics side, but rather a long list of challenges such as incorporation of multicomponent quark fields and non-Abelian plaquette terms in higher dimensions. A realistic pathway will be the investigation of increasingly complex (quantum link) models in an interplay between theory and experiment, with the short term goals of extending the present study to higher dimensions and in particular non-Abelian gauge field models.

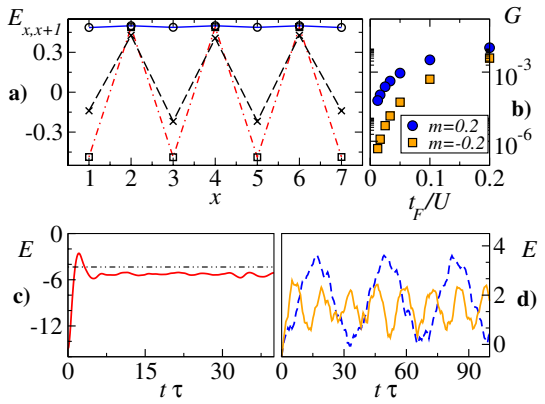

FIG. 3 (color online). (a) Flux configuration in the ground state of Eq. (4) compared to the QLM for $S = \frac{1}{2}$ obtained by exact diagonalization of an $L = 8$ site system. The parameters of the QLM (in units of $t_F = t_B = 1$) are $t = 0.05$, $\delta_F = -0.05$ (see Supplemental Material [33]), and $m = -0.2$, 0, 0.2 (squares, crosses, and circles). The corresponding microscopic parameters are $U = 20$ and $m = -0.2$, 0, 0.2 (dashed-dotted, dashed, and solid lines). (b) Accuracy of the effective gauge invariance parameter $G = \sum_x |\langle G_x \rangle|/L$ in the microscopic realization as a function of t_F/U. (c, d) Real-time evolution of the total electric flux $E = \sum_x E_{x,x+1}$ obtained by exact diagonalization of the QLM with $L = 16$. (c) For $S = 1$ (solid line) string breaking is illustrated, starting from the initial state at the top of Fig. 1(c), and approaching the corresponding vacuum expectation value (dashed-dotted line) of $E = \sum_x E_{x,x+1}$ ($g^2 = \sqrt{2}t > 0$, $m = 0$, $\delta_F = -\sqrt{2}t$; critical breaking length $L_c = 3$ when $t = 0$). (d) For $S = \frac{1}{2}$ we show the evolution after a quench, starting from the initial state at the top of Fig. 1(d). The flux order parameter performs coherent oscillations whose period and strength strongly depends on m ($m/t = 0.6(0.9)$ for dashed (thick) line, $\delta_F = 10t$).

We thank D. B. Kaplan, M. Lewenstein, B. Pasquiou, F. Schreck, and M. Zaccanti for discussions. P. Z. and M. D. thank the Joint Quantum Institute for hospitality.

Work at Bern is supported by the Schweizerischer Nationalfonds. Work at Innsbruck is supported by the integrated project AQUTE, the Austrian Science Fund through SFB F40 FOQUS, and by the DARPA OLE program. M. M. is supported by QUITEMAD S2009-ESP-1594, PICC: FP7 2007-2013 (Grant No. 249958) and MICINN Grant No. FIS2009-10061. Authors are listed in alphabetical order.

Note added.—While completing the present work, we became aware of two preprints [43,44] on atomic quantum simulation of $U(1)$ gauge theories (without coupling to fermions).

[1] M. Lewenstein, A. Sanpera, and V. Ahufinger, *Ultracold Atoms in Optical Lattices: Simulating Quantum Many-Body Systems* (Oxford University Press, New York, 2012).
[2] J. Cirac and P. Zoller, Nat. Phys. **8**, 264 (2012).
[3] I. Bloch, J. Dalibard, and S. Nascimbène, Nat. Phys. **8**, 267 (2012).
[4] R. Blatt and C. F. Roos, Nat. Phys. **8**, 277 (2012).
[5] K. Rajagopal and F. Wilczek, *Handbook of QCD*, edited by M. Shifman (World Scientific, Singapore, 2000).
[6] D. Horn, Phys. Lett. **100B**, 149 (1981).
[7] P. Orland and D. Rohrlich, Nucl. Phys. **B338**, 647 (1990).
[8] S. Chandrasekharan and U. J. Wiese, Nucl. Phys. **B492**, 455 (1997).
[9] K. Wilson, Phys. Rev. D **10**, 2445 (1974).
[10] R. Brower, S. Chandrasekharan, and U. J. Wiese, Phys. Rev. D **60**, 094502 (1999).
[11] R. Brower, S. Chandrasekharan, S. Riederer, and U. J. Wiese, Nucl. Phys. **B693**, 149 (2004).
[12] L. M. Duan, E. Demler, and M. D. Lukin, Phys. Rev. Lett. **91**, 90402 (2003).
[13] M. Hermele, M. P. A. Fisher, and L. Balents, Phys. Rev. B **69**, 064404 (2004).
[14] M. Levin and X. Wen, Rev. Mod. Phys. **77**, 871 (2005).
[15] H. P. Büchler, M. Hermele, S. D. Huber, M. P. A. Fisher, and P. Zoller, Phys. Rev. Lett. **95**, 40402 (2005).
[16] S. Tewari, V. W. Scarola, T. Senthil, and S. Das Sarma, Phys. Rev. Lett. **97**, 200401 (2006).
[17] H. Weimer, M. Müller, I. Lesanovsky, P. Zoller, and H. Büchler, Nat. Phys. **6**, 382 (2010).
[18] J. I. Cirac, P. Maraner, and J. K. Pachos, Phys. Rev. Lett. **105**, 190403 (2010).
[19] E. Kapit and E. Mueller, Phys. Rev. A **83**, 033625 (2011).
[20] M. Troyer and U. J. Wiese, Phys. Rev. Lett. **94**, 170201 (2005).
[21] S. Nascimbène, N. Navon, K. Jiang, F. Chevy, and C. Salomon, Nature (London) **463**, 1057 (2010).
[22] S. Trotzky, L. Pollet, F. Gerbier, U. Schnorrberger, I. Bloch, N. Prokof'ev, B. Svistunov, and M. Troyer, Nat. Phys. **6**, 998 (2010).
[23] K. Van Houcke, F. Werner, E. Kozik, N. Prokof'ev, B. Svistunov, M. Ku, A. Sommer, L. Cheuk, A. Schirotzek, and M. Zwierlein, Nat. Phys. **8**, 366 (2012).
[24] X. Zhang, C. Hung, S. Tung, and C. Chin, Science **335**, 1070 (2012).
[25] S. Trotzky, Y. Chen, A. Flesch, I. McCulloch, U. Schollwöck, J. Eisert, and I. Bloch, Nat. Phys. **8**, 325 (2012).
[26] D. Jaksch and P. Zoller, New J. Phys. **5**, 56 (2003).
[27] N. Goldman, A. Kubasiak, A. Bermudez, P. Gaspard, M. Lewenstein, and M. A. Martin-Delgado, Phys. Rev. Lett. **103**, 035301 (2009).
[28] Y. Lin, K. Jiménez-García, and I. Spielman, Nature (London) **471**, 83 (2011).
[29] J. Dalibard, F. Gerbier, G. Juzeliūnas, and P. Öhberg, Rev. Mod. Phys. **83**, 1523 (2011).
[30] M. Aidelsburger, M. Atala, S. Nascimbène, S. Trotzky, Y. A. Chen, and I. Bloch, Phys. Rev. Lett. **107**, 255301 (2011).
[31] N. R. Cooper, Phys. Rev. Lett. **106**, 175301 (2011).
[32] Gauge invariance in quantum mechanics with classical electromagnetic fields is discussed in C. Cohen-Tannoudji, B. Diu, and F. Laloë, *Quantum Mechanics* (Wiley, New York, 1977), Vol. 1, p. 315.
[33] See Supplemental Material at http://link.aps.org/supplemental/10.1103/PhysRevLett.109.175302 for an extended discussion.
[34] J. Kogut, Rev. Mod. Phys. **55**, 775 (1983).
[35] J. Kogut and L. Susskind, Phys. Rev. D **11**, 395 (1975).
[36] T. Banks, L. Susskind, and J. Kogut, Phys. Rev. D **13**, 1043 (1976).
[37] S. Coleman, Ann. Phys. (Berlin) **101**, 239 (1976).
[38] M. Pepe and U. J. Wiese, Phys. Rev. Lett. **102**, 191601 (2009).
[39] K. Rajagopal and F. Wilczek, Nucl. Phys. **B404**, 577 (1993).
[40] M. Anderlini, P. Lee, B. Brown, J. Sebby-Strabley, W. Phillips, and J. Porto, Nature (London) **448**, 452 (2007).
[41] S. Trotzky, P. Cheinet, S. Fölling, M. Feld, U. Schnorrberger, A. Rey, A. Polkovnikov, E. Demler, M. Lukin, and I. Bloch, Science **319**, 295 (2008).
[42] A. Auerbach, *Interacting Electrons and Quantum Magnetism* (Springer, New York, 1994).
[43] E. Zohar, J. Cirac, and B. Reznik, arXiv:1204.6574.
[44] L. Tagliacozzo, A. Celi, A. Zamora, and M. Lewenstein, arXiv:1205.0496.